

Some Features of the Phase Diagram of the Square Lattice $SU(N)$ Antiferromagnet

N. Read and Subir Sachdev

*Center for Theoretical Physics, P.O. Box 6666
and Section of Applied Physics, P.O. Box 2157
Yale University, New Haven, CT 06511*

ABSTRACT

We study the properties of the nearest neighbor $SU(N)$ antiferromagnet on a square lattice as a function of N and the number of rows (m) and columns (n_c) in the Young tableau of the $SU(N)$ representation on the A sublattice; the sites of the B sublattice have the conjugate representation (the familiar Heisenberg antiferromagnet has $N = 2$, $m = 1$ and $n_c = 2S$). We study the global phase diagram in the (N, m, n_c) space using $1/N$ expansions; in particular: (i) for N large with m proportional to N and n_c arbitrary, we find spin-Peierls (dimerized) ground states with short-range spin correlations; (ii) with $m = 1$, the model is shown to be equivalent, at order $1/N$, to a generalized quantum dimer model. We discuss the relationship of these results to the $SU(N)$ generalization of recent arguments by Haldane on the effect of ‘hedgehog’ point singularities in the space-time spin configuration. As an intermediate step in our calculation, we present a simple new derivation of the coherent state path integral representation of $SU(N)$ spin models.

PACS Nos. 75.10.Jm, 75.10.-b, 74.65.+n

September 27, 1988; submitted to Nucl. Phys. B

1. Introduction

The recent discovery of high temperature superconductivity in a class of cuprates compounds [1] has led to resurgence of interest in the properties of the $SU(2)$ Heisenberg antiferromagnet on a square lattice [2]. By a judicious choice of exchange constants, it may be possible for this model to have a ground state without long range Neel order. A complete understanding of the nature of these possible spin-disordered states is lacking, and reliable results on closely related, but tractable models will be useful. In this paper we discuss the nature of the global phase diagram of the $SU(N)$ generalization of the Heisenberg antiferromagnet. We will support our arguments by exact calculations in the $N \rightarrow \infty$ limit. We will also draw a connection between our results and a recent topological analysis of a semiclassical Heisenberg model by Haldane [3].

We will consider models obtained by generalizing the $SU(2)$ symmetry group of the Heisenberg antiferromagnet to $SU(N)$. This generalization can be viewed as an alternative to using, for example, non-nearest-neighbor interactions to move away from the Neel phase. This procedure yields a small number of well defined parameters which control the phases of the antiferromagnet. We shall study the Hamiltonian

$$H = \frac{J}{N} \sum_{(i,j)} \sum_{\alpha\beta} \hat{S}_{\alpha}^{\beta}(i) \hat{S}_{\beta}^{\alpha}(j) \quad (1.1)$$

where the \hat{S}_{α}^{β} are the generators of $SU(N)$, the Greek letters $\alpha, \beta = 1, \dots, N$ are the $SU(N)$ indices and sum over (i, j) extends over all near-neighbour pairs (referred to as ‘links’ in this paper). Closely related Hamiltonians have been examined earlier by Affleck [4], Affleck and Marston [5] and Arovas and Auerbach [6]. Our model is based upon the bipartite nature of the square lattice; at sites on sublattice A , say, we place a ‘spin’ transforming as a representation of $SU(N)$ represented by the Young tableau in Fig 1, which has $0 < m < N$

rows and n_c columns. On sites on sublattice B we place the conjugate representation which has $N - m$ rows. For $m = N/2$, the representations are self-conjugate and the model has greater translational symmetry. The choice of a rectangular Young tableau is for convenience; the choice of alternating conjugate representations is motivated by the fact that, among other things, the semiclassical limit is describable by a non-linear sigma ($NL\sigma$) model (Ref [7, 8] and Section 2). We emphasize that *the properties of H are completely determined once the representations of $SU(N)$ have been specified*. In particular the physics will be independent of whether we represent the generators by fermionic or bosonic operators. For the familiar Heisenberg antiferromagnet, $N = 2$, $m = 1$ and $n_c = 2S$ where S is the spin. For general N we find that n_c continues to play the role of twice the spin; the value of n_c will play a central role in determining the properties of the non-Neel ordered states that we find.

The phase diagram determined in this paper is shown in Fig 2 as a function of N and n_c ; the properties of the system are relatively insensitive to the value of m . There is a finite region in this plane where the Neel ground state is stable and the quantum fluctuations can be described semiclassically. A line of second order transitions separates the Neel phase from spin disordered states; for sufficiently large n_c or N , this line is shown in Section 2.2 to obey the equation $n_c = \kappa N$ where κ is a constant of order unity (this last result can also be obtained from the results of Ref [6] after proper identification of the $SU(N)$ representation).

The disordering effects of quantum fluctuations of the Neel order parameter were first given a field theoretic description by Haldane [7] for the case $N = 2$. The low energy, long wavelength dynamics of the system in or near a Neel phase on a d -dimensional (hyper-)cubic lattice can be described in the $SU(2)$ case by a $(d+1)$ dimensional $U(2)/(U(1) \times U(1))$ (or $O(3)$) $NL\sigma$ model [7, 8]. This model is known to possess a critical coupling constant $g = g_c$ (g depends upon S and the ratios of the various exchange constants [9]) above which

spin correlations decay exponentially; $g_c > 0$ for spatial dimension $d > 1$ while $g_c = 0$ in $d = 1$. The action for the spin system contains a Berry phase term which is responsible for the quantum nature of the spins; it gives rise in (1+1) dimensions to a topological term in the sigma model action which changes completely the low energy behavior of the system when the underlying spin at a site is half an odd integer [7, 8]. In (2+1) dimensions, on the other hand, the effect of the Berry phase term appears to be much more innocuous. Several investigators [3, 10] have noted that in this case the Berry phase term vanishes for any spin configuration in space and time in which the Neel order parameter is smooth on the scale of the lattice spacing. However, the recent work of Haldane [3], goes beyond this limitation by examining the effect of the Berry phase term evaluated on ‘hedgehog’ point singularities in the 2+1 dimensional spin configuration. While the Neel phase was unaffected, the quantum interference between various hedgehog configurations led Haldane to predict that the properties of the disordered phase of the $NL\sigma$ model depended crucially upon the value of $2S(\text{mod } 4)$. His results can be used to argue that *all* low-lying states in the disordered phase have a degeneracy of *at least* 1,4,2, and 4 for values of $2S(\text{mod } 4)$ of 0,1,2, and 3 respectively. This is reminiscent of the result of Lieb-Schultz-Mattis [11] theorem for the $d = 1$ models which states that a degeneracy of at least 1,2 exists for $2S(\text{mod } 2) = 0, 1$ respectively.

In this paper we shall examine in (2+1) dimensions for *general* N , n_c and m (*i*) the nature of the transition from the Neel phase to the disordered phase and (*ii*) the structure of the disordered phase. The main results we shall establish are

1. For *large* n_c ($n_c \rightarrow \infty$ with N, m fixed) the $SU(N)$ antiferromagnets behave semiclassically and are described by a $U(N)/(U(m) \times U(N - m))$ $NL\sigma$ model [8]. Below a critical value of $n_c \sim \kappa N$, the $NL\sigma$ model is in a disordered phase. The arguments

of Haldane [3] on ‘hedgehog’ singularities have a simple generalization to these models and lead to the conjecture that the *all* low lying states in the disordered phase of the $SU(N)$ antiferromagnets have a degeneracy of *at least* 1,4,2, and 4 for values of $n_c(\text{mod } 4)$ of 0,1,2, and 3 respectively.

2. We determine the nature of the disordered phase in two different large N limits. The first type of $1/N$ expansion is defined by taking $N \rightarrow \infty$ with m of order N and n_c fixed. We find various ‘ground’ states, which are either stable, global minima or metastable minima; all the states have short-range spin correlations, and broken translational symmetry (with the exception of a metastable state for $n_c(\text{mod } 4) = 0$.) All of the states have a degeneracy which is consistent with the lower limit determined in the semiclassical $NL\sigma$ model: *i.e.* all states have a degeneracy greater than 1,4,2, and 4 for $n_c(\text{mod } 4) = 0,1,2$, and 3 respectively. The global ground states have a degeneracy of 4 for all values of n_c . Among the metastable states is a sequence which saturates the lower bound on the degeneracy:*i.e.* these states have a degeneracy of exactly 1,4,2, and 4 for $n_c(\text{mod } 4) = 0,1,2$, and 3 respectively.
3. The second $1/N$ expansion takes $N \rightarrow \infty$ with $m = 1$ and n_c fixed. The model is shown at order $1/N$ to be exactly equivalent to a generalized quantum dimer model. Preliminary numerical results indicate that this particular dimer model possesses crystalline ground states which do not violate the degeneracy bound suggested by the $NL\sigma$ model. On the other hand, Rokhsar and Kivelson [12] have conjectured for the case $n_c = 1$, that the dimer model has a resonating valence bond liquid phase. Such a phase may still have a degeneracy consistent with the bound [13] even though the ground state is translationally invariant.

4. As an intermediate step towards establishing (1), we will present a simple new derivation of the coherent state path integral for $SU(N)$ spin models.

In the remainder of this section we establish the formalism which will be used throughout and outline the techniques by which the various results are obtained. The $1/N$ expansions we shall consider are most conveniently generated by using the following fermionic representation of the generators of $SU(N)$:

$$\hat{S}_\alpha^\beta(i) = \sum_a c_{\alpha a}^\dagger(i) c^{\beta a}(i) - \delta_\alpha^\beta \frac{n_c}{2} \quad (1.2)$$

in terms of the ‘electron’ destruction operators $c_{\alpha a}$. In addition to the $SU(N)$ index, the electrons also carry an additional color index represented by the the Latin letters $a, b = 1, \dots, n_c$ where n_c is the number of colors. The \hat{S} operators are not traceless; the reason for the particular trace chosen will become clear in Section 2. The electron states are restricted to be color singlets upon each site by the constraint

$$\sum_\alpha c_{\alpha a}^\dagger c^{\alpha b} = \begin{cases} \delta_a^b m & \text{on sublattice } A \\ \delta_a^b (N - m) & \text{on sublattice } B \end{cases} \quad (1.3)$$

There are thus a total of mn_c ($(N - m)n_c$) electrons on sublattice A (B). It is easy to show that the representation (1.2) and the constraint (1.3) restricts the Hilbert space on each site to the representations of $SU(N)$ represented by the Young tableau of Fig 1, *i.e.* m rows and n_c columns on sublattice A and $N - m$ rows and n_c columns on sublattice B . For the special case of $SU(2)$ these representations are both equivalent to spin $S = n_c/2$.

We emphasize that we could equally well have represented the generators of $SU(N)$ in terms of boson creation and destruction operators for all values of m , N and n_c . In this case the representation for the A sublattice is $\hat{S}_\alpha^\beta = b_{\alpha p}^\dagger b^{\beta p}$ where the $b_{\alpha p}^\dagger$ operators are boson creation operators carrying the $SU(N)$ index α and the ‘‘color’’ index p which extends over the range $1, \dots, m$. When combined with the constraint $\sum_\alpha b_{\alpha p}^\dagger b^{\alpha q} = \delta_p^q n_c$

we obtain the $SU(N)$ representation with n_c columns and m rows. On the B sublattice the bosons transform as the conjugate representation of $SU(N)$, but the constraints are otherwise unaltered. These representations are useful in taking the alternative large N limit, $N \rightarrow \infty$ with $n_c \propto N$ and m fixed as in Ref [6]; this is denoted by the arrow labelled AA in Fig 2.

Two different methods are used to generate a $1/N$ expansion of the disordered phase of the $SU(N)$ antiferromagnet. These methods will be illustrated by examining the values (a) $m = N/2$ and (b) $m = 1$. For case (a) a functional integral decoupling method is most convenient while for case (b) each successive order of ordinary Rayleigh-Schrödinger perturbation theory generates a higher power of $1/N$. We now briefly describe our results for these models.

(a) $m = N/2$

We use the functional integral decoupling method used by a number of investigators for the Kondo problem [14] and antiferromagnets [5]. At leading order ($N = \infty$), a very large set of degenerate ground states was found for $n_c = 1$ [5] and we find a similar situation for all n_c . These states are ‘dimerized’, *i.e.* they consist of a covering of the lattice with $SU(N)$ singlet bonds, n_c bonds ending at each lattice site. To split the degeneracy, we calculate $1/N$ correction; these generate bond-configuration-dependent terms in the energy of these states, which pick out a definite arrangement of bonds in each case. We find that the lowest energy for all n_c occurs when the n_c bonds ending at a site coincide, and these sets of n_c bonds are arranged in columns (Fig 3a). Thus these states are four-fold degenerate for all n_c . However, there are other metastable states (Fig 3b-d) which exist for particular values of $n_c \pmod{4}$ and which give lower degeneracy. In particular, we may spread the bonds as uniformly as possible, by placing p bonds on every link, and arranging the remaining k bonds (for $n_c = 4p+k$, $0 \leq k < 4$) as in Figs 3a-d. These metastable states saturate the conjectured

lower bound on the degeneracy of 1,4,2,4 for $n_c(\text{mod } 4) = 0,1,2,3$ respectively. No low-lying states which violate this lower bound are found.

(b) $m = 1$

The case $m = 1$ for one-dimensional chains has been considered previously by Affleck [4]. The Rayleigh-Schrödinger perturbation expansion used there can be easily applied to the square lattice in the limit $m \ll N$. There are however some minor errors in the structure of the perturbation expansion presented by Affleck (the correction of these errors leaves the physics of the model considered by Affleck unchanged). It will be important to correct these errors for the case of the square lattice. We show that at order $1/N$ the system can be described by an effective generalized dimer model. For $n_c = 1$ this dimer model is a special case of the quantum dimer model considered by Rokhsar and Kivelson [12]; however unlike Ref [12] our class of models are applicable to all n_c and we are able to determine exactly the values of the parameters in the effective Hamiltonian in terms of J . We have determined the ground state of our dimer Hamiltonian (see Eqn 4.10) for $n_c = 1$ upon a 6×6 lattice with periodic boundary conditions by the Lanczos method; these finite size calculations show a clear indication of a crystalline ground state with the symmetry of Fig 3a.

The outline of the remainder of the paper is as follows. In Section 2 we will present a simple new derivation of a coherent state path integral representation of $SU(N)$ spin models. This representation is used in the large n_c limit to derive a $NL\sigma$ model representation of $SU(N)$ antiferromagnets. The coherent state representation also yields a Berry phase term in the action; we then generalize Haldane's [3] arguments for $SU(2)$ to show that this Berry phase term is non-zero only for the $SU(N)$ generalization of 'hedgehog' point singularities; the phases associated with the hedgehogs suggest a degeneracy of all low-lying states of at least 1,4,2, or 4 depending upon whether $n_c(\text{mod } 4) = 0,1,2, \text{ or } 3$. Some details of this

argument are relegated to the appendix. Sections 3 and 4 move away from the semiclassical limit ($n_c \gg 1$) to the extreme quantum limit ($N \gg n_c$). Section 3 discusses the case $m = N/2$, while Section 4 discusses $m = 1$. We conclude in Section 5 with a discussion of the implication of our results for the $SU(2)$ Heisenberg antiferromagnet.

2. Semiclassical Theory

In this section we shall extend the results obtained by Haldane [3] in the large spin limit of $SU(2)$ antiferromagnets to $SU(N)$. The antiferromagnets behave semiclassically when n_c is large, and the quantum fluctuations are described by a $U(N)/(U(m) \times U(N - m))$ $NL\sigma$ model. We shall begin, in Section 2.1, with an exact path-integral representation of the partition function of $SU(N)$ quantum spins. The semiclassical limit of this path integral will be used to derive the $NL\sigma$ model and associated Berry phase terms in Section 2.2.

2.1 Path Integral Representation of $SU(N)$ Spins

The standard method for deriving the path integral representation of a quantum problem proceeds by deriving the coherent state representation of the Hilbert space [15]; we will follow this method here. We first define the Cartan subalgebra $\{H_\alpha\}$ of $SU(N)$ by choosing the operators

$$H_\alpha = \hat{S}_\alpha^\alpha = \sum_a c_{aa}^\dagger c^{aa} - \frac{n_c}{2} \quad (2.1)$$

Notice that we have dropped the site index i . For the time being we consider sites on sublattice A only; the modification for sublattice B will be given at the end of the subsection. The remaining \hat{S}_α^β operators with $\alpha \neq \beta$ are the ‘raising’ and ‘lowering’ operators which complete the canonical Cartan basis for the Lie algebra. The coherent state basis is obtained

by unitary transformations upon the highest weight state $|\Psi_0\rangle$ defined as follows

$$|\Psi_0\rangle = C \left[\epsilon^{ab\dots} c_{\lambda a}^\dagger c_{\lambda b}^\dagger \dots \right] \left[\epsilon^{cd\dots} c_{\rho c}^\dagger c_{\rho d}^\dagger \dots \right] \dots |0\rangle \quad (2.2)$$

where there are n_c electron creation operators within each square bracket, and the square bracketed terms appear m times; C is a normalization constant. The indices λ, ρ, \dots run through all the indices between 1 and m . The weight of this state is given by

$$H_\alpha |\Psi_0\rangle = \begin{cases} (n_c/2) |\Psi_0\rangle & \text{if } \alpha \in [1, m] \\ -(n_c/2) |\Psi_0\rangle & \text{if } \alpha \in [m+1, N] \end{cases} \quad (2.3)$$

The coherent states for the rectangular $m \times n_c$ Young tableau are defined as follows [16]

$$|q\rangle = \exp \left(q_\mu^\lambda \hat{S}_\lambda^\mu - q_\mu^{\lambda*} \hat{S}_\mu^\lambda \right) |\Psi_0\rangle \quad (2.4)$$

where as above, the index λ runs through the values $[1, m]$, and μ runs through $[m+1, N]$; these limits on λ and μ will be implicitly assumed in the rest of this section. The q_μ^λ are $m(N-m)$ independent complex numbers. The states $|q\rangle$ are normalized to unity and obey the following important identity

$$\langle q | \hat{S}_\alpha^\beta | q \rangle = \frac{n_c}{2} Q_\alpha^\beta \quad (2.5)$$

where the matrix Q is defined by the relationship

$$Q = U \Lambda U^\dagger \quad (2.6)$$

The unitary matrix U represents the action of the unitary transformation in equation (2.4) upon the fundamental representation and is given by

$$U = \exp \left[\begin{pmatrix} 0 & q \\ -q^\dagger & 0 \end{pmatrix} \right] \quad (2.7)$$

where q is a $m \times (N-m)$ matrix with elements q_μ^λ . The constant matrix Λ is given by

$$\Lambda = \begin{pmatrix} 1_m & 0 \\ 0 & -1_{N-m} \end{pmatrix} \quad (2.8)$$

where 1_r is a $r \times r$ unit matrix. The matrix Q therefore satisfies $Q^2 = 1$ and extends over the manifold $U(N)/(U(m) \times U(N - m))$.

The standard method of coherent state quantization [15] may now be used to obtain the following representation for the partition function

$$Z = \int \mathcal{D}Q(\tau) \exp \left\{ \int_0^\beta d\tau \left[\frac{\langle q(\tau) | q(\tau + \delta\tau) \rangle - 1}{\delta\tau} - H(Q(\tau)) \right] \right\} \quad (2.9)$$

where $H(Q)$ is obtained by replacing every occurrence of \hat{S}_α^β in the Hamiltonian by $(n_c/2)Q_\alpha^\beta$, $Q(0) = Q(\tau)$, and $\mathcal{D}Q(\tau)$ is the invariant measure over the $U(N)/(U(m) \times U(N - m))$ manifold. It now remains to evaluate the first term in the action, S_B , the Berry phase term. Using Eqn (2.4) and the following identity for the derivative of the exponential of any operator M [17]

$$\frac{d}{dx} e^M = \int_0^1 du e^{M(1-u)} \frac{dM}{dx} e^{Mu} \quad (2.10)$$

we may easily show that

$$S_B = \int_0^\beta d\tau \int_0^1 du \langle \Psi_0 | \exp \left(-u(q_\mu^\lambda \hat{S}_\lambda^\mu - q_\mu^{\lambda*} \hat{S}_\mu^\lambda) \right) \left(\frac{\partial q_\mu^\lambda}{\partial \tau} \hat{S}_\lambda^\mu - \frac{\partial q_\mu^{\lambda*}}{\partial \tau} \hat{S}_\mu^\lambda \right) \exp \left(u(q_\mu^\lambda \hat{S}_\lambda^\mu - q_\mu^{\lambda*} \hat{S}_\mu^\lambda) \right) | \Psi_0 \rangle \quad (2.11)$$

Using the fundamental property of the coherent states in Eqn. (2.5) the above expression reduces immediately to

$$S_B = \frac{n_c}{2} \int_0^\beta d\tau \int_0^1 du \left[\frac{\partial q_\mu^\lambda}{\partial \tau} Q_\lambda^\mu(\tau, u) - \frac{\partial q_\mu^{\lambda*}}{\partial \tau} Q_\mu^\lambda(\tau, u) \right] \quad (2.12)$$

where we have now introduced a u and τ dependent matrix Q which is defined as in Eqn (2.6) in terms of the unitary matrix $U(\tau, u)$

$$U = \exp \left[u \begin{pmatrix} 0 & q(\tau) \\ -q^\dagger(\tau) & 0 \end{pmatrix} \right] \quad (2.13)$$

As a function of u , Q therefore satisfies $Q(\tau, 0) = \Lambda$ and $Q(\tau, 1) \equiv Q(\tau)$. We may now integrate Eqn (2.12) by parts and obtain the simple expression

$$S_B = -\frac{n_c}{2} \int_0^\beta d\tau \int_0^1 du \text{Tr} \left[\begin{pmatrix} 0 & q(\tau) \\ -q^\dagger(\tau) & 0 \end{pmatrix} \partial_\tau Q(\tau, u) \right] \quad (2.14)$$

Using the easily established identity

$$\begin{pmatrix} 0 & q(\tau) \\ -q^\dagger(\tau) & 0 \end{pmatrix} = -\frac{1}{2} Q(\tau, u) \frac{\partial Q(\tau, u)}{\partial u} \quad (2.15)$$

we obtain our final result for the action of the path integral

$$S = \int_0^\beta d\tau \int_0^1 du \left[\frac{n_c}{4} \text{Tr} \left(Q(\tau, u) \frac{\partial Q(\tau, u)}{\partial u} \frac{\partial Q(\tau, u)}{\partial \tau} \right) \right] - \int_0^\beta d\tau H(Q(\tau)) \quad (2.16)$$

A similar result has been quoted recently by Wiegmann [18].

The derivation above uses a very specific dependence of Q upon u in Eqn (2.13). This form satisfies the boundary conditions

$$Q(\tau, 0) = Q(\tau', 0) \text{ for all } \tau, \tau' \quad (2.17)$$

$$Q(\tau, 1) = Q(\tau) \quad (2.18)$$

$$Q(0, u) = Q(\beta, u) \quad (2.19)$$

which means that the rectangle $0 \leq \tau \leq \beta$, $0 \leq u \leq 1$ over which Q varies can be regarded as a disc with $u = 1$ as the boundary, on which $Q = Q(\tau)$. Thus the parametrization in (2.13) is just a specific way of filling in the closed curve $\{Q(\tau) : 0 \leq \tau \leq \beta\}$ to form a disc in $G(m, N) = U(N)/(U(m) \times U(N - m))$. We now show that any other surface with this boundary gives the same value of S_B up to addition of a term $2\pi n_c k i$ for some integer k . This result uses crucially the fact that $\pi_2(G(m, N)) = Z$, the group of integers, and that this is also equal to the second cohomology group $H^2 = Z$ (by the Hurewicz isomorphism theorem); the integrand of S_B when integrated *over a sphere* is the integral invariant associated with

both of these groups. We use the representation

$$S_B = \frac{n_c}{8} \int d^2\zeta \varepsilon_{pq} \text{Tr}(Q\partial_p Q\partial_q Q) \quad (2.20)$$

where p, q take the values 1, 2, $\zeta_1 = \tau$ and $\zeta_2 = u$, and the integral is over a rectangular in (τ, u) space. We parametrize

$$Q(\tau, u) = U(\tau, u)\Lambda U^\dagger(\tau u) \quad (2.21)$$

where U is a smooth function on the rectangle and can be taken to obey the boundary conditions (2.19). Using Stokes theorem, we obtain

$$S_B = \frac{n_c}{2} \oint d\zeta_p \text{Tr}(\Lambda U^\dagger \partial_p U) = \frac{n_c}{2} \int_0^\beta d\tau \text{Tr}(\Lambda U^\dagger(\tau) \partial_\tau U(\tau)) \quad (2.22)$$

where $U(\tau) = U(\tau, 1)$ Now we may leave $Q(\tau)$ unchanged by right multiplying U by a unitary matrix U_0 also satisfying the conditions (2.19) and for $u = 1$ satisfying $U_0\Lambda U_0^\dagger = \Lambda$. The change in the Berry phase due to U_0 is seen to be

$$\Delta S_B = n_c \int_0^\beta d\tau A_\tau \quad (2.23)$$

where we have introduced the abelian gauge field $A_\tau = (1/2)\text{Tr}(\Lambda U_0^\dagger \partial_\tau U_0)$ which is a pure gauge when $u = 1$. The constraint on U_0 for $u = 1$ restricts U_0 to $U(m) \times U(N - m)$ and implies

$$U_0 = \begin{pmatrix} U_{0a} & 0 \\ 0 & U_{0b} \end{pmatrix} \quad \text{for } u = 1 \quad (2.24)$$

where U_{0a} (U_{0b}) is a $m \times m$ ($(N - m) \times (N - m)$) unitary matrix. We now find

$$\Delta S_B = n_c \int_0^\beta d\tau \frac{1}{2} \frac{\partial}{\partial \tau} [\ln \det U_{0a} - \ln \det U_{0b}] \quad (2.25)$$

With the periodic boundary condition $U_0(0) = U_0(\beta)$ this integral is easily seen to be an integer multiple of $\pi n_c i$. However since U and hence U_0 is supposed to be defined over the

disc (rectangle) $0 \leq \tau \leq \beta$, $0 \leq u \leq 1$, $\det U$ is smooth and vanishes nowhere. Then on the boundary $u = 1$, the phase of $\det U$ cannot wind by 2π since this would force $\det U$ to vanish somewhere in the interior by continuity. Then $\det U_0$ cannot wind either, which implies that

$$\int_0^\beta d\tau \frac{\partial}{\partial \tau} [\ln \det U_{0a} + \ln \det U_{0b}] = 0 \quad (2.26)$$

Using this constraint, ΔS_B is now seen to be an integer multiple of $2\pi n_c i$. Thus the exponential of S_B is unaffected by the change in parametrization of U . Incidentally this shows that the parameter n_c must be integer valued; this is in direct analogy to the quantization of flux for a monopole, which implies the quantization $2S = \text{integer}$ in the $SU(2)$ case [19]. Indeed, the form (2.22) has precisely the form of a line integral of a vector potential, so that the Berry phase is the integral of a ‘flux’ over a surface spanned by the curve $Q(\tau)$; in earlier derivations [7, 10] for $SU(2)$ this vector potential was introduced explicitly. This makes clear the connection with H^2 also, since the ‘magnetic field’ is a rank 2 antisymmetric tensor on $G(m, N)$ of non-zero cohomology class.

On sublattice B , we have the conjugate representation, so in Eqn (2.2) we have instead $(N - m)$ square brackets. It is convenient for describing the classical Neel state to take the highest weight state to have the indices λ, ρ, \dots running between $m + 1$ and N in this case, so that

$$H_\alpha |\Psi_0\rangle = \begin{cases} -(n_c/2) |\Psi_0\rangle & \text{if } \alpha \in [1, m] \\ (n_c/2) |\Psi_0\rangle & \text{if } \alpha \in [m + 1, N] \end{cases} \quad (2.27)$$

Then use of the same matrix q_μ^λ as before gives

$$\langle q | \hat{S}_\alpha^\beta | q \rangle = -\frac{n_c}{2} Q_\alpha^\beta \quad (2.28)$$

and S_B has the opposite sign as before. Thus in a classical Neel state, Q is the Neel order parameter which is *uniform* in space. In the next subsection, we derive the $NL\sigma$ model describing long-wavelength excitations in this representation, together with ‘hedgehogs’.

2.2 Non-linear Sigma Model Representation

In the large n_c limit, the antiferromagnet behaves semiclassically, and we may decompose the Q field fluctuations into staggered and uniform components

$$Q(i) \approx \Omega_i \sqrt{1 - a^2 L_i^2} + \eta_i a L_i \quad (2.29)$$

where η_i equals +1 on sublattice A and -1 on sublattice B , a is the lattice spacing, $\Omega_i^2 = 1$, and L_i is small and satisfies $L_i \Omega_i + \Omega_i L_i = 0$. Substituting this into Eqn (2.16), dropping total time derivatives and taking the continuum limit following Refs [3] and [8] we obtain

$$S = S'_B + \frac{1}{2} \int_0^\beta d\tau \int d^2x \text{Tr} \left[\frac{Jn_c^2}{4N} (\nabla_x \Omega)^2 + \frac{2Jn_c^2}{N} L^2 - \frac{n_c}{2a} L \Omega \partial_\tau \Omega \right] \quad (2.30)$$

where

$$S'_B = i n_c \sum_j \eta_j \omega_j \quad (2.31)$$

is defined in terms of the spatial field ω_j

$$\omega_j = \frac{1}{4i} \int_0^\beta d\tau \int_0^1 du \text{Tr} [\Omega_j \partial_u \Omega_j \partial_\tau \Omega_j] \quad (2.32)$$

We may now integrate out the L fluctuations and obtain the action of a (2+1) $NL\sigma$ model with a residual Berry phase term

$$S = S'_B + \frac{1}{2} \int_0^\beta d\tau \int d^2x \frac{\rho_s}{2} \text{Tr} \left[(\nabla_x \Omega)^2 + \frac{1}{c^2} (\partial_\tau \Omega)^2 \right] \quad (2.33)$$

where we have introduced the spin-wave stiffness $\rho_s = Jn_c^2/2N$ and the spin-wave velocity $c = \sqrt{8}Jn_c a/N$. (For the case of $SU(2)$ we may make substitutions $\Omega = n_\alpha \sigma^\alpha$, $N = 2$ and $n_c = 2S$ where n_α is a unit 3-vector and σ_α are the Pauli matrices; the action then reduces to the 0(3) $NL\sigma$ model with the spin-wave stiffness and velocity having their standard values.)

Before discussing topological effects of the residual Berry phase we present results on the stability of the Neel phase. Following the analysis of Ref [9] and [20] we introduce the

coupling constant $g = (c/\rho_s)k_M = 4\sqrt{2}k_M a/n_c$, where k_M is an upper cutoff in momentum space, and derive the following one-loop renormalization group equation in a $(d-1)$ expansion

$$\frac{dg}{dl} = -(d-1)g + \frac{N}{4}K_d g^2 \quad (2.34)$$

where $d = 2$ is the spatial dimensionality, e^l is the length rescaling factor, and $K_d = 1/(2^{d-1}\pi^{d/2}\Gamma(d/2))$ is a numerical constant. This equation predicts that the Neel phase will be stable provided $g < 4/(NK_d)$ or

$$n_c > (K_d\sqrt{2}\pi k_M a)N \quad (2.35)$$

This determines a line of second-order transitions in the (N, n_c) plane across which the Neel phases transforms into a phase with exponentially decaying spin correlations. This transition is represented by the dashed line in Fig 2. Note that, at one-loop order, the position of the line is independent of m .

As an alternative to the $(d-1)$ expansion we may examine the $NL\sigma$ model field theory in the large N limit. Taking the limit with m and Ng fixed (implying $n_c \sim N$) the renormalization group equation (2.34) is in fact exact. For sufficiently large N therefore the statements of the previous paragraph have a validity beyond a $(d-1)$ expansion. Alternatively, as explained in Section 1, one can use the bosonic representation of the generators \hat{S}_α^β in the Hamiltonian (1.1) and perform a $1/N$ expansion directly on the quantum spin system. This was done in Ref [6] for the case $m = 1$ where, indeed, a transition to a disordered state at $T = 0$ was found at a critical value of $n_c/N \simeq 0.2$. Thus there is a close connection between the results of Refs [9] and [6].

We now turn to a discussion of the effects of the Berry phase term S'_B on this transition. The residual Berry phase has been shown to vanish [10] for any order parameter configuration which is smooth on the scale of the lattice spacing. Following Ref [3], it is therefore

necessary to consider space-time singularities in the order parameter. The order-parameter configuration for each constant time slice can be characterized by a ‘skyrmion’ number associated with $\pi_2(U(N)/(U(m) \times U(N - m)))$ [21]. Non-trivial contributions to S'_B arise only from tunneling events which change the number of skyrmions; these tunneling events must necessarily be associated with space-time point singularities in the order parameter field $\Omega(x, \tau)$. We show in the appendix that the singularity, associated with a tunneling event which changes the skyrmion number by Δn_s , is a vortex of magnitude $2\pi\Delta n$ in the spatial field ω_j . The remaining arguments are unchanged from the $SU(2)$ case [3]. The cuts accompanying the vortex in the field ω_j yield the phase factor

$$(\xi_j)^{n_c\Delta n} \tag{2.36}$$

in the action for the tunneling event which changes the skyrmion number by Δn ; here ξ_j is $+1$, -1 , $+i$, or $-i$ depending upon whether the vortex is centered on a plaquette with (even,even), (odd,odd), (even,odd) or (odd,even) co-ordinates. For $n_c(\text{mod } 4) = 1$ or 3 , the phase factor ξ_j will lead to destructive interference between tunneling events except those involving a change in the skyrmion number Δn which is a multiple of 4. This suggests that the Hilbert space of the system splits up into 4 separate sectors characterized by the number of skyrmions modulo 4, with vanishing tunneling matrix elements between the sectors. In the Neel phase there is a finite energy gap towards the creation of skyrmions, and therefore this argument only affects some high lying states. In the massive phase however, the skyrmions proliferate, and this argument suggests a *minimum* degeneracy of *all* low-lying states of 4. In a similar manner we can argue that, in the spin-disordered phase for $n_c(\text{mod } 4) = 2$, all low-lying states have a degeneracy of at least 2. The degeneracy can be arbitrarily small for $n_c(\text{mod } 4) = 0$.

We conclude this section with a reiteration of the main results established. We have

shown that in the semiclassical (large n_c) limit, the $SU(N)$ spin model is described by a $NL\sigma$ model. At a value of $n_c = \kappa N$ (where κ is a constant of order 1) the Neel phase undergoes a second order phase transition to a state with exponentially decaying spin correlations. This massive phase was argued to have a degeneracy of all low-lying states of at least 1,4,2, or 4 as $n_c \pmod{4}$ took the values 0,1,2, or 3.

3. Functional Integral Method

This section will analyze the properties of the Hamiltonian (1.1) for the case $m = N/2$, n_c arbitrary but small, in the large N limit. This is most conveniently done by using the fermion representation in Eqn (1.2). The resulting interacting fermion theory can be analyzed by the functional integral method developed for the heavy-fermion problem [14] and used in the context of the $SU(N)$ antiferromagnets by Affleck and Marston [5]. While the method can in principle be used for any m of order N the $m = N/2$ case has a particle-hole symmetry which simplifies the calculation. Attempts by Marston and Affleck [22] to use the functional integral method for the case $m = 1$ have apparently not led to a consistent $1/N$ expansion. This case will be addressed in Section 4 by different methods.

Generalizing the procedure of Ref [5] to n_c colors, the fermion interaction can be decoupled by introducing a $n_c \times n_c$ matrix field $\chi_b^a(ij)$ on every link (i, j) ; the a, b are color indices. It is easy to show that the partition function for Hamiltonian H in Eqn (1.1) can be expressed as follows (after subtracting a constant energy of $-Jn_c^2/2$ per site):

$$Z/Z_o = \int_{-\pi/\beta}^{\pi/\beta} \frac{d\lambda_b^a(i)}{2\pi} \int \mathcal{D}c\mathcal{D}c^\dagger\mathcal{D}\chi \exp\left(-\int_0^\beta d\tau \mathcal{L}(\tau)\right) \quad (3.1)$$

where the Lagrangian \mathcal{L} is given by

$$\mathcal{L} = c_{\alpha a}^\dagger(i) \frac{\partial c^{\alpha a}(i)}{\partial \tau} + i\lambda_b^a(i) \left[c_{\alpha a}^\dagger(i) c^{\alpha b}(i) - \delta_a^b N/2 \right] + \frac{N}{J} |\chi_b^a(ij)|^2$$

$$+ c_{\alpha\alpha}^\dagger(i)c^{\alpha b}(j)\chi_b^a(ij) + \chi_a^b(ji)c_{\alpha b}^\dagger(j)c^{\alpha a}(i) \quad (3.2)$$

with all repeated indices summed over. The normalization Z_o is given by

$$Z_o = Z_F \int \mathcal{D}\chi \exp\left(-\int_0^\beta d\tau |\chi_b^a(ij)|^2\right) \quad (3.3)$$

where Z_F is a free fermion determinant.

The structure of the theory is straightforward in the large N limit. After integrating out the fermions, the effective action for the χ and λ fields acquires a factor of N in front. The functional integral can therefore be approximated by the stationary phase point of the action. By particle-hole symmetry the expectation value of the λ fields is zero at the stationary phase point. In addition it can easily be shown the fluctuations of the λ fields make no contribution to the ground state energy; the λ field will therefore be omitted in the subsequent discussion. The effective action for the χ fields after integrating out the fermions is given by

$$\frac{S_{eff}}{N} = \int_0^\beta d\tau \left[-\text{Tr} \text{Ln} \left(\frac{\partial}{\partial \tau} \delta_b^a \delta_{ij} + \chi_b^a(ij) \right) + \frac{1}{J} \sum_{\langle ij \rangle} \sum_{ab} |\chi_b^a(ij)|^2 \right] \quad (3.4)$$

with $\chi_b^a(ij) = (\chi_a^b(ji))^*$.

A class of time-independent stationary phase solutions of S_{eff} are those with χ color-diagonal. The colors then decouple from each other and the subsequent minimization becomes identical to the one color calculation carried out by Affleck and Marston. The global minima found by Affleck and Marston correspond to the ‘bond’ solutions: for each color, a , the field $\chi_a^a(ij)$ has a mean field value of either $\bar{\chi}$ or 0 on every link ($\bar{\chi} = J/2$ at this order); every site has exactly one link with $\chi_a^a = J/2$ (a ‘bond’) for all values of the color a . The relative positions of bonds with different colors is however arbitrary. The ground state energy E_G is given by

$$E_G = -\frac{N_s N n_c J}{8} \quad (3.5)$$

where N_s is the number of sites on the square lattice.

There is an additional continuous family of solutions to the mean field equations which was not considered by Affleck and Marston and which is degenerate with the ‘bond’ states in the $n \rightarrow \infty$ limit. This family is illustrated in Fig 4 for the color a . The lattice splits into disjoint plaquettes, with the mean field values of χ_a^a nonzero only along the links surrounding the plaquette. The constraints satisfied by the values of χ_a^a on a plaquette of sites numbered 1,2,3,4 (Fig 4) are

$$|\chi_a^a(12)| = |\chi_a^a(34)| \quad ; \quad |\chi_a^a(41)| = |\chi_a^a(23)| \quad ; \quad |\chi_a^a(12)|^2 + |\chi_a^a(23)|^2 = J^2/4$$

$$\chi_a^a(12)\chi_a^a(23)\chi_a^a(34)\chi_a^a(41) = -|\chi_a^a(12)|^2|\chi_a^a(23)|^2 \quad (3.6)$$

A special case of this mean field solution was found in Ref [23]. Note that by choosing $\chi_a^a(41) = \chi_a^a(23) = 0$, the ‘plaquette’ states reduce to a subset of the ‘bond’ states. We will show in the next subsection, that the $1/N$ corrections pick out a particular bond configuration as the lowest energy state.

Going beyond the assumption of color-diagonal solutions, we have carried out an extensive computer search for additional time independent χ configurations which minimize S_{eff} with up to three colors. We examined all periodic configurations with a unit cell of four sites. No additional color-gauge inequivalent solutions with a lower energy were found for any n_c studied, and we believe that none exist for any n_c .

3.1 $1/N$ Corrections for $n_c = 1$

To break the degeneracy in the ground state it is necessary to consider the $1/N$ corrections to the ground state energy. The analysis is simplest for the one color case which will be considered first. We will refer to the color by the index a , and will therefore focus on the

fluctuations of $\chi_a^a(ij)$. We will present details of the calculation for the ‘bond’ states. The calculations for the ‘plaquette’ states can be carried out in a similar manner.

The contributions to the effective action can be divided into two classes: the link-diagonal and off-diagonal terms. Consider first the link-diagonal terms. Let B_a be the set of links in a given mean-field configuration which has a bond of color a on it. The set B'_a is the complement of B_a . The link diagonal contributions to S_{eff} can be shown to equal

$$\begin{aligned} \Delta^1 S_{eff}^{aa} &= \sum_{(i,j)} \frac{N}{\beta} \sum_n \chi_a^a(ij; \omega_n) \chi_a^a(ji; -\omega_n) \left(\frac{1}{J} - \frac{\bar{\chi}}{\omega_n^2 + 4\bar{\chi}^2} \right) \\ &+ \sum_{(i,j) \in B_a} \frac{N}{\beta} \sum_n (\chi_a^a(ij; \omega_n) \chi_a^a(ij; -\omega_n) + \chi_a^a(ji; \omega_n) \chi_a^a(ji; -\omega_n)) \frac{\bar{\chi}/2}{\omega_n^2 + 4\bar{\chi}^2} \end{aligned} \quad (3.7)$$

where we have introduced the Fourier transformed variables $\chi_b^a(ij; \omega_n)$ as a function of the Matsubara frequency $\omega_n = 2\pi n/\beta$ for integer n , and the first summation extends over all the sites of the square lattice.

As the fermion fluctuations are localized upon the bonds, it easy to see that there is only one type of local bond configuration which leads to an off diagonal coupling: this configuration is shown in Fig 5. There is a bond of color a on link (1,2) and also on link (3,4); the fermion fluctuations will lead to coupling between $\chi_a^a(13)$ and $\chi_a^a(24)$. Such terms to lead to the following additional terms in the effective action

$$\Delta^2 S_{eff}^{aa} = \sum_{(i,j) \in B_a; (k,l) \in B_a} \frac{N}{\beta} \sum_n (\chi_a^a(ki; \omega_n) \chi_a^a(jl; -\omega_n) + \chi_a^a(ik; \omega_n) \chi_a^a(lj; -\omega_n)) \frac{\bar{\chi}}{\omega_n^2 + 4\bar{\chi}^2} \quad (3.8)$$

where, naturally, (i, k) and (j, l) have to be links of the square lattice.

The functional integral over the $\chi_a^a(ij)$ variables can now be carried out as the action is quadratic. The structure of the resulting determinant is sufficiently local that it can be evaluated for *any* random bond configuration. After determining the correction to the value

of $\bar{\chi}$, we obtain the following ground state energy at order $1/N$

$$\Delta E_G(n_c = 1) = -N_a \frac{J}{2} - N_{\parallel} \frac{J}{2} - N_r \frac{J}{2} (2 - \sqrt{2}) \quad (3.9)$$

The first term arises from the links with a bond on them; N_a is the number of links in B_a . The second term arises from parallel bond pairs like the ones shown in Fig 5; N_{\parallel} is the number of links in B'_a belonging to such configurations. The third term is contribution of the remaining N_r links. We therefore have the constraint $N_a + N_{\parallel} + N_r = 2N_s$. Examining equation (3.9), we see that parallel pairs of bonds lower the ground state energy because the absolute value of the coefficient of N_{\parallel} is larger than that of N_r . This picks out four-fold degenerate ‘column’ states (shown in Fig 3a), which maximize the number of parallel bonds, as the lowest energy ‘bond’ state ($\Delta E_G = -N_s J(5 - \sqrt{2})/4$).

We also need the $1/N$ corrections for the energy of ‘plaquette’ states. These can be evaluated using methods similar to the ones presented in this subsection. The results obviously depend upon the mean field values of χ_a^a on the plaquettes which can now vary continuously between 0 and $J/2$. We have verified that at order $1/N$ the ‘column’ state has the lowest energy among this entire class of solutions. For example, the correction to the energy of the state shown in Fig 4 with $|\chi_a^a| = J/(2\sqrt{2})$ on all the links on the plaquettes is $\Delta E_G = -N_s J(5 - \sqrt{3})/4$. The column state is therefore identified as the true ground state of H for $n_c = 1$. Note however that the column state can be transformed continuously to a ‘plaquette’ state, indicating the presence of gapless singlet excitations. There is clearly a gap towards excitations transforming as higher representations of $SU(N)$ because it is necessary to destroy a singlet bond to create them.

3.2 $1/N$ corrections for $n_c \geq 2$

The fluctuation corrections to the ground state energy for all $n_c \geq 2$ can be performed using a method similar to that of the previous section. The color diagonal fluctuations $\chi_a^a(ij)$ do not mix with each other and lead to a simple sum of n_c contributions of the one color result. The color off-diagonal fields $\chi_b^a(ij)$ couple just the 2 colors a and b ; we therefore obtain $n_c(n_c - 1)/2$ similar contributions of two color fluctuations. We will only consider the ‘bond’ states in this section as the color-diagonal fluctuations have lowered their energy below the ‘plaquette’ states.

It is clear, therefore, that all that remains to be calculated are the contributions due to the fluctuations of the field $\chi_b^a(ij)$, with $a \neq b$ being two fixed colors. We now enumerate the various contributions to the action for the colors a and b .

(i) There is one link diagonal term which occurs on all links of the lattice

$$\Delta^1 S_{eff}^{ab} = \sum_{(i,j)} \frac{N}{\beta} \sum_n (\chi_b^a(ij; \omega_n) \chi_a^b(ji; -\omega_n) + \chi_a^b(ij; \omega_n) \chi_b^a(ji; -\omega_n)) \left(\frac{1}{J} - \frac{\bar{\chi}}{\omega_n^2 + 4\bar{\chi}^2} \right) \quad (3.10)$$

(ii) A second link-diagonal term occurs on links which have bonds of both colors a and b (Fig 6a):

$$\Delta^2 S_{eff}^{ab} = \sum_{(i,j) \in B_a; (i,j) \in B_b} \frac{N}{\beta} \sum_n (\chi_b^a(ij; \omega_n) \chi_a^b(ij; -\omega_n) + \chi_b^a(ji; \omega_n) \chi_a^b(ji; -\omega_n)) \frac{\bar{\chi}}{\omega_n^2 + 4\bar{\chi}^2} \quad (3.11)$$

(iii) One off-diagonal term occurs when a bond of color a and a bond of color b have just one site in common (Fig 6b):

$$\Delta^3 S_{eff}^{ab} = \sum_{(i,j) \in B_a; (j,k) \in B_b} \frac{N}{\beta} \sum_n (\chi_b^a(ij; \omega_n) \chi_a^b(kj; -\omega_n) + \chi_b^a(ji; \omega_n) \chi_a^b(jk; -\omega_n)) \frac{\bar{\chi}}{\omega_n^2 + 4\bar{\chi}^2} \quad (3.12)$$

(*iv*) and the other off-diagonal term occurs when a bond of color a is parallel to a bond of color b (Fig 6c):

$$\Delta^4 S_{eff}^{ab} = \sum_{(i,j) \in B_a; (k,l) \in B_b} \frac{N}{\beta} \sum_n (\chi_b^a(ik; \omega_n) \chi_a^b(lj; -\omega_n) + \chi_a^b(ki; \omega_n) \chi_b^a(jl; -\omega_n)) \frac{\bar{\chi}}{\omega_n^2 + 4\bar{\chi}^2} \quad (3.13)$$

where (i, k) and (j, l) must be links of the square lattice.

The action for n_c colors can now be constructed from the expressions above. The functional integral and the resulting determinant can easily be evaluated for an arbitrary configuration of bonds by a simple extension of the one color results. We will omit the intermediate steps and simply present the results for the energy of the lowest metastable states and ground states for small n_c .

(a) One Dimension

We begin the discussion by considering first the one-dimensional chain. For $n_c = 2$, there are only two possible ground states: one in which the two colors alternate from link to link, and the other in which they overlap. These configurations are shown in Fig 7. The energy of the ‘alternating’ state is $-N_s J(N/4 + (5 - \sqrt{2})/2)$ while that of the ‘overlapping’ state is $-N_s J(N/4 + (6 - 2\sqrt{2})/2)$. The ground state is therefore the non-degenerate alternating state, which bears a close resemblance to the states considered by Affleck [4] for $m = 1$. Interchanging the position of the color in the alternating state produces a state which is color-gauge equivalent to the original state; the alternating state is therefore non-degenerate. The ground state for arbitrary n_c is now clear: for even n_c we have a unique ground state in which the colors split into two groups which alternate with each other; for odd n_c we have a two-fold degenerate ground state with the even links having one less or more bond than the odd links.

We emphasize that, for the first time in a functional integral large- N expansion, we have obtained for n_c even (S integral for $N = 2$) a unique ground state separated by a gap (the Haldane [7] gap) from the low-lying spin excitations, which will be in the adjoint or singlet representations of $SU(N)$. We will now argue that our result for n_c odd (half-integer S for $N = 2$) of a pair of degenerate ground states, which break translational symmetry and have a gap for (soliton-like, fundamental representation) excitations, is *usually* the physically correct result. This is in contrast to the discussion of Arovas and Auerbach [6], who studied the $n_c = 1$ case and found a spatially *uniform* saddle point solution, which gives gapless, Fermi-liquid like excitations. Their result is attractive because for $N = 2$, $S = 1/2$ it agrees with the correct physics known since Bethe's solution [25]. There are nonetheless difficulties with this point of view, the first of which is that the saddle point is unstable; the energy can be continuously lowered [26] until the dimerized state is reached, due to a Peierls instability of the Fermi 'surface'. Further, using the analogue of this state for arbitrary n_c , one apparently obtains a (gapless) constrained Fermi system that corresponds to the Wess-Zumino-Witten (WZW) model with $k = n_c$ [8]. The WZW model has different properties for the cases $N = 2$ and $N > 2$: (a) $N = 2$ The correct result for this model is believed [27] to be that n_c even leads to ground states with a gap, and n_c odd leads to leads to an $SU(2)$ WZW model with $k = 1$, *i.e.* the same exponents as $n_c = 1$. The crossover from $k = n_c$ to $k = 1$ (for n_c odd) apparently occurs because the conformal $SU(2)$ WZW field theory with $k > 1$ possesses relevant operators which generically have non-zero coefficients (say for the Heisenberg model), causing a runaway from $k = n_c$ [27]. (b) $N > 2$ The WZW model has relevant operators for *all* $k \geq 1$ and a gapless Fermi phase is expected only at isolated (multicritical) points in the Hamiltonian parameter space, which presumably do not coincide with the model here studied. Hence one expects that, for n_c even the ground state

is translationally invariant and has a gap, and for n_c odd [28] translational symmetry is broken, *i.e.* a spin-Peierls phase. It is quite satisfying that the large- N theory agrees with this.

As noted above, for $N = 2$ there should be gapless behavior similar to the known exact result for $n_c = 1$ [25] for all odd $n_c \geq 1$. To obtain such behavior in a functional integral type of approach at least involves, for $n_c = 1$, somehow stabilizing the uniform solution, and for larger n_c , finding a crossover away from the $k = n_c$ saddle point behavior to an effective $k = 1$.

(b) Two Dimensions

We now return to our discussion of the square lattice. We first restrict our attention to $n_c = 2$. The three lowest gauge inequivalent metastable states can be shown to be the ones in Fig 8; we shall refer to these states as the four-fold degenerate ‘overlapping’ state (Fig 8a), the two-fold degenerate ‘line’ state (Fig 8b), and the four-fold degenerate ‘square’ state (Fig 8c). (Note that the line state in Fig 8b is an alternative representation of the state in Fig 3b of the introduction.) Because of the enhanced interference between the two colors, the ‘overlapping’ state turns out to have the lowest energy $-N_s J(N/4 + 5 - \sqrt{2})$. The ‘square’ state and the ‘line’ state turn out to have the same energy $-N_s J(N/4 + (11 - 3\sqrt{2})/2)$; we however do not expect these states to be degenerate when higher order terms in $1/N$ are included. The ‘square’ state and the ‘line’ state are also metastable towards deformation to the ‘overlapping’ state: performing local bond rearrangements to transform between the states always creates higher energy intermediate states. Thus for $n_c = 2$ we have found a four-fold degenerate ground state (the overlapping state of Fig 8a), and the two lowest metastable states - the two-fold degenerate line state (Fig 8b) and the four-fold degenerate square state (Fig 8c). All three states have a degeneracy greater than the lower bound

suggested by the $NL\sigma$ model in Section 2.2, with the degeneracy of the line state being the lowest allowed value of 2.

There is now a straightforward prescription for generating the lowest metastable states for *any* n_c . (i) Arrange all the bonds of a given color into column states; the relative orientation of the column states of different colors can be arbitrary. The contribution of the fluctuations of the color-diagonal field $\chi_a^a(ij)$ to the energy will be simply n_c times the one-color contribution of Section 3.1 (ii) Take all $n_c(n_c - 1)/2$ possible combinations of two color pairs. The two colors chosen (a and b say) will necessarily form either the overlapping state, the square state or the line state and the fluctuations of the $\chi_b^a(ij)$ field will give the corresponding contribution to the energy. It is now easy to show that *all* such states have a degeneracy (after excluding color gauge equivalent states) of at least 1,4,2,4 for $n_c \pmod{4} = 0,1,2,3$ respectively. This is one of the central results of this paper. Thus, for example, it is impossible to obtain a state with a degeneracy smaller than 4 for $n_c = 5$. The states which have the smallest possible degeneracy for all n_c were displayed in Fig 3. The global ground state for all n_c is formed when all of the colors overlap in the same column state; this state is therefore the $n_c > 2$ generalization of Fig 8a and is four-fold degenerate.

We have therefore determined the ground states and the lowest metastable states for all n_c of the $m = N/2$ models. None of the states obtained violate the lower bound on the ground state degeneracy of 1,4,2,4 for $n_c \pmod{4} = 0,1,2,3$ respectively, which was suggested by the semiclassical $NL\sigma$ model Section 2.2.

4. Mapping to a Generalized Dimer Model

In this section we will consider properties of the Hamiltonian in Eqn (1.1) for the case $m = 1$. Using the fermion representation of Eqn (1.2) for the $SU(N)$ generators we now find that

there are n_c electrons per site on the A sublattice and $(N - 1)n_c$ electrons per site on the B sublattice. We will show that for $m = 1$, at order $1/N$, the antiferromagnet is exactly equivalent to a generalized quantum dimer Hamiltonian. The $m = 1$ antiferromagnet has in fact already been considered by Affleck [4] in one dimension, where the dimer Hamiltonian is trivially solvable. While the overall phase diagram obtained by Affleck is correct, there are some minor errors in the structure of his perturbation theory; it will be important to correct these errors to understand the physics in two dimensions.

We begin by describing the model with $n_c = 2$, but we shall use a general formalism which will allow a straightforward generalization to arbitrary n_c . It is convenient to make a particle-hole transformation on the B sublattice by introducing the hole operators $\tilde{c}_{\alpha a} = c_{\alpha a}^\dagger$; on this sublattice we also use conjugate $SU(N)$ generators

$$\hat{S}_\alpha^\beta(i) = \sum_a \tilde{c}^{\beta a \dagger}(i) \tilde{c}_{\alpha a}(i) - \delta_\alpha^\beta \frac{n_c}{2} \quad (4.1)$$

which are (-1) times the usual generators. The vacuum state is now redefined to have no electrons on the A sublattice and no holes on the B sublattice; all physical states will have n_c electrons per site on the A sublattice and n_c holes per site on the B sublattice. We also introduce the symmetric tensor operators $T_{\alpha\beta}$

$$T_{\alpha\beta}(i) = \epsilon_{ab} c_{\alpha a}^\dagger(i) c_{\beta b}^\dagger(i) \quad (4.2)$$

on every site on the A sublattice. On the B sublattice, the $\tilde{T}^{\alpha\beta}(j)$ operators are defined identically, with the \tilde{c}^\dagger operators replacing the c^\dagger operators. The Hilbert space is spanned by the action of the T operators upon the vacuum state on every site of the square lattice. (For arbitrary $n_c > 2$ we generalize these operators to symmetric tensor operators $T_{\alpha\beta\gamma\dots}$, with n_c free $SU(N)$ indices, by using a n -th rank Levi-Civita antisymmetric tensor $\epsilon_{abc\dots}$ in color space.)

In the $N \rightarrow \infty$ limit the ground states of H can be easily deduced from the arguments of Affleck [4]. The ground state has a degeneracy of order $\exp(cN)$ for some constant c . Each ground state can be described as follows: contract the $SU(N)$ indices of the $T_{\alpha\beta}$ on neighbouring sites in an arbitrary manner until there are no free indices left. All of the states so obtained are manifestly $SU(N)$ singlets and can be labelled by a set of non-negative integers, $\{n_\ell\}$, where $0 \leq n_\ell \leq n_c$ is the number of contractions ('bonds') on the link ℓ of the square lattice. For example, the state

$$|\cdots n_{(i,j)} \cdots n_{(p,q)}, n_{(q,r)}, n_{(r,s)}, n_{(s,p)} \cdots\rangle = C' \left(\sum_{\alpha\beta\gamma\delta\nu\sigma} \cdots T_{\alpha\beta}(i) \tilde{T}^{\alpha\beta}(j) \cdots T_{\gamma\delta}(p) \tilde{T}^{\delta\nu}(q) T_{\nu\sigma}(r) \tilde{T}^{\sigma\gamma}(s) \cdots \right) |0\rangle \quad (4.3)$$

where C' is a normalization constant, (i, j) , (p, q) , (q, r) , (r, s) and (s, p) are links of the square lattice, has $n_{(i,j)} = 2$, and $n_{(p,q)} = n_{(q,r)} = n_{(r,s)} = n_{(s,p)} = 1$. The set of integers $\{n_\ell\}$ must also satisfy the constraint

$$n_{(i,i+\hat{x})} + n_{(i,i-\hat{x})} + n_{(i,i+\hat{y})} + n_{(i,i-\hat{y})} = n_c \quad (4.4)$$

because there are n_c $SU(N)$ indices emerging from each site (the sum in the equation above extends over the four links ending at the site i).

A word is in order here about our phase convention for the states. We will always write the $T_{\alpha\beta\dots}(i)$ operators by using a *fixed*, but arbitrary, ordering of the sites i of the square lattice. This convention now uniquely determines the state $|\{n_\ell\}\rangle$ once the values of the link variables n_ℓ are known. We show in Fig 9 sample ground states in $N \rightarrow \infty$ limit for a few n_c values. The integers on the links specify the number of $SU(N)$ bonds between the two sites at the ends of the links.

4.1 Order $1/N$

We now show that at order $1/N$, there are matrix elements which mix the states in the ground state manifold; this mixing can be described by an effective Hamiltonian which is a generalization of the quantum dimer Hamiltonians considered by Rokhsar and Kivelson [12].

The results follow from the repeated use of the following commutation relation

$$[\hat{S}_\alpha^\beta, T_{\gamma\delta}] = T_{\gamma\alpha}\delta_\delta^\beta + T_{\delta\alpha}\delta_\gamma^\beta \quad (4.5)$$

and its obvious generalization to arbitrary n_c . A similar result holds on sublattice B . The site index has been suppressed in the above two equations. To evaluate the energy of the bonds between the sites i and j we will need the following commutator

$$\begin{aligned} & \left[\hat{S}_\mu^\nu(i) \hat{S}_\nu^\mu(j), T_{\alpha\beta}(i) T^{\gamma\delta}(j) \right] = \\ & \delta_\alpha^\gamma T_{\mu\beta}(i) \tilde{T}^{\mu\delta}(j) + \delta_\alpha^\delta T_{\mu\beta}(i) \tilde{T}^{\mu\gamma}(j) + \delta_\beta^\gamma T_{\alpha\mu}(i) \tilde{T}^{\mu\delta}(j) + \delta_\beta^\delta T_{\alpha\mu}(i) \tilde{T}^{\mu\gamma}(j) \\ & + \left\{ T_{\mu\beta}(i) \tilde{T}^{\gamma\delta}(j) \hat{S}_\alpha^\mu(j) + T_{\alpha\mu}(i) \tilde{T}^{\gamma\delta}(j) \hat{S}_\beta^\mu(j) + T_{\alpha\beta}(i) \tilde{T}^{\mu\delta}(j) \hat{S}_\mu^\gamma(i) + T_{\alpha\beta}(i) \tilde{T}^{\gamma\mu}(j) \hat{S}_\mu^\delta(i) \right\} \end{aligned} \quad (4.6)$$

This result can be used to commute the Hamiltonian H in Eqn (1.1) through the T operators, and so determine the diagonal energies and the off-diagonal mixing terms between the states $|\{n_\ell\}\rangle$. The terms in the curly brackets in Eqn (4.6) annihilate the ground state and can be ignored in the subsequent discussion. The remaining terms in Eqn (4.6) have three different types of effects:

(i) They contribute a diagonal term to the energy of the state $|\{n_\ell\}\rangle$. The contribution of a n_ℓ -fold bond on a link, E_{n_ℓ} , to the ground state energy can easily be computed to be

$$E_{n_\ell} = -\frac{J}{N} n_\ell (N - 1 + 2n_c - n_\ell). \quad (4.7)$$

In Eqn (4.7), and in the remainder of this section, we have omitted a constant energy per site of $(Jn_c^2/2)(1 - 4m/N)$.

(ii) They generate states which have a bond between the sites which are *not* nearest neighbors. An example of this process is illustrated in Fig 10 for the case $n_c = 1$. It is easy to show that such processes contribute to the energy of states $|\{n_\ell\}\rangle$ in second order perturbation theory. They shift the energy of the states by an amount proportional to

$$J \frac{m^2(N - m)^2}{N^2(N - 1)^2}. \quad (4.8)$$

For $m = 1$, this contribution is proportional to $1/N^2$, and can therefore be neglected. For m of order N however, these terms are of the *same* order as the first order perturbation theory result. This makes clear why the calculations of this section do not define a consistent perturbation theory for $m = N/2$, and the functional integral method of Section 3 is the appropriate way to proceed.

(iii) They lead to mixing between the states $|\{n_\ell\}\rangle$, as shown in Fig 11. The action of the Hamiltonian leads to a local rearrangement in the values of the n_ℓ field around a plaquette. A plaquette with $n_1, n_2 - 1, n_3, n_4 - 1$ bonds on the four links around it can be transformed to a configuration with $n_1 - 1, n_2, n_3 - 1, n_4$ bonds on the links. The matrix element for the process requires determination of the normalization constant C' , and use of Eqn (4.6); it can be shown to equal

$$\langle \cdots n_1, n_2 - 1, n_3, n_4 - 1 \cdots | H | \cdots n_1 - 1, n_2, n_3 - 1, n_4 \cdots \rangle = -(2J/N) \sqrt{n_1 n_2 n_3 n_4} \quad (4.9)$$

We are now in a position to express the $1/N$ corrections in terms of a effective Hamiltonian H_{eff} acting upon the Hilbert space of the $|\{n_\ell\}\rangle$ states. The non-orthogonality of the different $|\{n_\ell\}\rangle$ states can be shown to affect H_{eff} only at order $1/N^2$. Using the results in Eqn (4.4),

(4.7), and (4.9) we can show

$$\begin{aligned} \frac{H_{eff}}{J/N} &= \sum_{\{n_\ell\}} |\{n_\ell\}\rangle \left(\sum_\ell n_\ell^2 \right) \langle \{n_\ell\} | \\ &- \sum_{\ell_1, \ell_2, \ell_3, \ell_4 \in \square} |\cdots n_{\ell_1}, n_{\ell_2} - 1, n_{\ell_3}, n_{\ell_4} - 1, \cdots\rangle 2\sqrt{n_{\ell_1} n_{\ell_2} n_{\ell_3} n_{\ell_4}} \langle \cdots n_{\ell_1} - 1, n_{\ell_2}, n_{\ell_3} - 1, n_{\ell_4}, \cdots | \end{aligned} \quad (4.10)$$

where the second sum extends over all plaquettes on the lattice. Equation (4.10) defines the effective Hamiltonian of the generalized dimer model. Notice that while the full Hamiltonian was not invariant under translation by one lattice spacing, the “reduced” dimer Hamiltonian (4.10) does have this property. For $n_c = 1$, it reduces to a special case of the quantum dimer model of Ref [12]. In one dimension, the off-diagonal term vanishes and H_{eff} is trivially soluble. The ground states, as noted by Affleck [4], for even n_c are non degenerate and have $n_\ell = n_c/2$ on every link of the chain. (For $N = 2$ these states are identical to the exact ground states of the models introduced in Ref [24]) For odd n_c , the ground states have a two-fold degeneracy and we have $n_\ell = (n_c + 1)/2$ on even links and $n_\ell = (n_c - 1)/2$ on odd links or vice versa. H_{eff} differentiates the candidate states obtained from the $N \rightarrow \infty$ limit at order $1/N$, whereas Affleck incorrectly found a difference only at order $1/N^2$.

The physics of H_{eff} is not so transparent in two dimensions. The first term in Eqn (4.10) is clearly minimized if the n_ℓ values on all the links are as equal as possible, subject to the constraint in Eqn (4.4). Thus for $n_c(\text{mod } 4) = 0$, the first term is minimized by the translationally invariant state with $n_\ell = n_c/4$ on all the links; this will be equivalent to the state shown in Fig 3d. However there is the possibility that the off-diagonal terms do not pick out a state with broken translational symmetry as the ground state. For other values of $n_c(\text{mod } 4) \neq 0$, one clearly can construct crystalline states similar to the ones in Fig 3a, 3b, and 3c, but it is not a priori obvious that they will have a lower energy than a state in which the dimers have melted into a translationally invariant fluid state. We note

however, as shown by Read and Chakraborty [13], that translationally invariant fluid states can also have a non-trivial ground state degeneracy. In any case, the $d = 2$ version of the Lieb-Schultz-Mattis theorem [11], which applies to a translationally-invariant Hamiltonian (which for us means *only* if either $m = N/2$ or $N = 2$) on a lattice with an odd number of rows, demands that the ground state have either gapless excitations or at least a 2-fold degeneracy if n_c is odd.

We have carried out preliminary numerical calculations of H_{eff} for the case $n_c = 1$. Using the Lanczos method, we were able to determine the exact ground state of H_{eff} on a 6×6 lattice with periodic boundary conditions. The bond correlation functions in these small lattices show a clear signal of a crystalline ground state with the symmetry of the state in Fig 3a (the correlation functions appear to reach their asymptotic values within two lattice spacings, indicating that finite size effects are small). Further details on the numerical calculations will be published in a separate paper.

5. Conclusion

The $NL\sigma$ model representation of the Heisenberg antiferromagnet (ignoring momentarily the effect of Berry phase terms) predicts two classes of ground states for $d > 1$ for fairly general spin Hamiltonians [9]: (i) a Goldstone phase with long-range Neel order and spin-wave fluctuations and (ii) some sort of massive phase with exponentially decaying spin correlations. Power law spin correlations are only allowed at special critical points separating the phases. However, the underlying quantum spin Hamiltonian can introduce a Berry phase term in the action, which can potentially change the nature of the massive phase. In one dimension, no ordered phase can exist, and here the effect of such a residual Berry phase term (the θ term [7, 8]) is dramatic: as noted first by Haldane [7], in the $SU(2)$ case for half-integer

spins, gapless excitations carrying spin-1/2 appear and give power law spin correlations, in contrast to the integer spin case, where the only excitations are massive and carry integer spin. The exact solution for the spin-1/2 antiferromagnetic chain [25] helped motivate these results, which are also supported by numerical studies [29] and can be given a field-theoretic interpretation [8, 27]. (The somewhat different situation for $N > 2$ was discussed in Section 3.) Thus the combination of arguments based on the $NL\sigma$ model representation (obtained in the semiclassical large S limit) with other results appears to predict the correct physics down to $S = 1/2$ in one spatial dimension.

The effect of the Berry phase term on the $NL\sigma$ model in two spatial dimensions however appears to be much more innocuous [3]. It does not affect the low energy dynamics of the Neel phase, changing only the structure of some high energy excitations. In the massive phase, Haldane [3] has suggested that it leads to additional degeneracies in low-lying states which depend on $2S(\text{mod } 4)$. We have obtained, in this paper, results in the extreme quantum limit ($N \rightarrow \infty$) of a nearest neighbor $SU(N)$ spin model which support the correctness of this conjecture. For the case when the number of rows, m , in the Young tableau of the $SU(N)$ representation satisfies $m = N/2$, we find massive ground states which break translational symmetry. The degeneracy of all of the low-lying states is always 4, exceeding the conjectured lower bound of degeneracy 1, 4, 2, or 4 for $n_c(\text{mod } 4) = 0, 1, 2$, or 3 respectively (here n_c is the number of columns in the Young tableau of the $SU(N)$ representation under consideration). Our results lead us to conjecture that the ground state anywhere in the disordered region of the phase diagram, Fig 2, is a dimerized (spin-Peierls) state similar to one of those in Fig 3, and satisfying the conjectured lower bound on the ground state degeneracy (we regard a non-degenerate state like Fig 3d as a spin-Peierls state also). This region may contain other phase boundaries which are transitions among spin-Peierls states of different degeneracies, and it

is amusing to speculate that Haldane's lower bound is saturated adjacent to the transition to Neel order, but that the degeneracy and hence the degree of breakdown of translational invariance tends to increase as we move away from this region, until the extreme region (N large, n_c fixed) studied in this paper is reached. Thus we expect that, once again, the semiclassical picture leads to qualitatively correct results even for small values of n_c . However, we emphasise that our results are for the unfrustrated nearest-neighbor model and that the introduction of large amounts of frustration or of mobile holes may lead to quite different disordered phases.

Acknowledgements

The authors benefitted greatly from discussions with R. Shankar. We would like to thank A. Manohar for useful comments. We are grateful to the Aspen Center for Physics and IBM Thomas J. Watson Research Center for hospitality while this work was being performed. S.S. was supported in part by the Presidential Young Investigators program of the National Science Foundation.

Appendix

This appendix fills in some missing steps in the arguments of Section 2.2 on the $NL\sigma$ model representation of the $SU(N)$ model. We shall show that a tunneling event which changes the skyrmion number by p leads to a vortex of magnitude $2\pi p$ in the spatial field ω_j which was defined in Eqn (2.32). For simplicity we will restrict our attention to the $U(N)/(U(1) \times U(N-1))$ models, also known as the Cp^{N-1} models. Our results can easily be generalized to the $U(N)/((U(m) \times U(N-m)))$ models by the methods of MacFarlane [30]. We begin with the following representation of the matrix field Ω_j

$$(\Omega_j)_{\alpha\beta} = \delta_{\alpha\beta} - 2Z_\alpha^*(j)Z_\beta(j) \quad (\text{A.1})$$

where $Z_\alpha(j)$ are N complex fields ($\alpha = 1, \dots, N$) satisfying the constraint $\sum_\alpha |Z_\alpha|^2 = 1$. Inserting this equation into Eqn (2.32) we can show easily

$$\omega_j = -i \int_0^\beta d\tau \sum_\alpha Z_\alpha^*(j) \frac{dZ_\alpha(j)}{d\tau} \quad (\text{A.2})$$

We will describe the evolution of the Z_α variables during a skyrmion-number changing tunneling event which is centered at the origin. We will focus of the four points, z_{1-4} shown in Fig 12, at the vertices of the plaquette where the tunneling occurs; here $z_j = x_j + iy_j$ are the complex co-ordinates of the points. Let us begin at time $\tau = 0$ with a skyrmion centered at the origin. The order parameter field for this can be written in the form [31]

$$Z_\alpha(j) = \frac{\hat{U}_\alpha + \hat{V}_\alpha(z_j/\lambda)^p}{\sqrt{1 + (|z_j|/\lambda)^{2p}}} \quad (\text{A.3})$$

where λ is a length, much larger than the lattice spacing a , specifying the scale of the skyrmion, and \hat{U}_α and \hat{V}_α are orthogonal unit vectors in the N dimensional order parameter space. It is convenient to break up the subsequent time evolution of the Z_α fields into four steps:

(i) *Step 1: $0 < \tau < \tau_1$*

The tunneling occurs in this step, reducing the skyrmion number to 0. The order parameter has the following time dependence

$$Z_\alpha(j, \tau) = \frac{\hat{U}_\alpha + \hat{V}_\alpha f(\tau)(z_j/\lambda)^p}{\sqrt{1 + f^2(\tau)(|z_j|/\lambda)^{2p}}} \quad (\text{A.4})$$

where $f(\tau)$ is a *real* function of time satisfying $f(0) = 1$ and $f(\tau_1) = \Gamma$; Γ is a large constant which satisfies $\lambda/\Gamma \ll a$. At $\tau = \tau_1$, the scale of the skyrmion is λ/Γ which is much smaller than the lattice spacing; consequently the skyrmion number has been reduced to 0. By inserting Eqn (A.4) into Eqn (A.2) we can easily see that the contribution of this step to ω_j is zero at all sites.

(ii) *Step 2: $\tau_1 < \tau < \tau_2$*

To satisfy periodic boundary conditions, we have to now return the order parameter configuration at the points z_{1-4} to their $\tau = 0$ values in a *locally smooth* manner; this will be achieved in Steps 2 and 3. We first rotate the order parameter configurations at z_{1-4} to a common value :

$$Z_\alpha(j, \tau) = \frac{\hat{U}_\alpha + \hat{V}_\alpha g_j(\tau)\Gamma(z_j/\lambda)^p}{\sqrt{1 + |g_j(\tau)|^2\Gamma^2(|z_j|/\lambda)^{2p}}} \quad (\text{A.5})$$

where $g_j(\tau_1) = 1$, and $g_j(\tau_2) = (z_j^*)^p/|z_j|^p$. Since the absolute values $|z_j|$ are equal at the four points under consideration, at $\tau = \tau_2$ the order parameters are also equal. This step involves a non-trivial Berry phase factor; we may show by inserting Eqn (A.5) into Eqn (A.2) that

$$\omega_j = -i \int_{\tau_1}^{\tau_2} d\tau \frac{\Gamma^2(|z_j|/\lambda)^{2p}}{1 + |g_j(\tau)|^2\Gamma^2(|z_j|/\lambda)^{2p}} \frac{1}{2} \left[g_j^*(\tau) \frac{dg_j(\tau)}{d\tau} - c.c. \right] \quad (\text{A.6})$$

In the limit $\lambda/\Gamma \ll a$, the integral can be easily evaluated and we obtain $\omega_1 = 0$, $\omega_2 = p\pi/2$, $\omega_3 = p\pi$, and $\omega_4 = 3p\pi/2$.

(iii) *Steps 3 and 4: $\tau_2 < \tau < \beta$*

These steps are the reverse of steps 1 and 2. Step 3 undoes the scale contraction in step 1 and gives no additional contribution to ω_j . Step 4 is the reverse of the rotation carried out in step 2; it is easy to check that, because $z_j \ll \lambda$, there is no additional contribution to ω_j .

All of the Berry phase contribution in the tunneling event therefore arose in Step 2. It is clear from the values of ω_j quoted above that a vortex of magnitude $2\pi\rho$ was generated at the origin. We have therefore established the required result.

Bibliography

- [1] J.G. Bednorz and K.A. Muller, Z. Phys. **B64**, 188 (1986); M.K. Wu *et. al.*, Phys. Rev. Lett. **58**, 908 (1987).
- [2] P.W. Anderson, Science **235**, 1196 (1987).
- [3] F.D.M. Haldane, Phys. Rev. Lett. **61**, 1029 (1988)
- [4] I. Affleck, Phys. Rev. Lett. **54**, 966 (1985).
- [5] I. Affleck and J. Brad Marston, Phys. Rev. **B37**, 3774 (1988).
- [6] D.P. Arovas and A. Auerbach, Phys. Rev. **B38**, 316 (1988); Phys. Rev. Lett. **61**, 617 (1988).
- [7] F.D.M. Haldane, Phys. Lett. **93A**, 464 (1983); Phys. Rev. Lett. **50**, 1153 (1983); and J. Appl. Phys. **57**, 3359 (1985).
- [8] I. Affleck, Nucl. Phys. **B257**, 397 (1985); Nucl. Phys. **B265**, 409 (1985).
- [9] S. Chakravarty, B.I. Halperin, and D.R. Nelson, Phys. Rev. Lett., **60**, 1057 (1988).
- [10] X.G. Wen and A. Zee, Phys. Rev. Lett., **61**, 1025 (1988); E. Fradkin and M. Stone, Phys. Rev. B to be published; T. Dombre and N. Read, to be published; R. Shankar and S. Sachdev, unpublished.

- [11] E. Lieb, T. Schultz, and D. Mattis, Ann. Phys. (N.Y.) **16**, 407 (1961); I. Affleck and E. Lieb, Lett. Math. Phys. **12**, 57 (1986); I. Affleck, Phys. Rev. **B37**, 5186 (1988).
- [12] D. Rokhsar and S. Kivelson, preprint.
- [13] N. Read and B. Chakraborty, preprint.
- [14] N. Read and D.M. Newns, J. Phys. C **16**, 3273 (1983); N. Read, J. Phys C **18**, 2651 (1985).
- [15] *Coherent States* by J.R. Klauder and B. Skagerstam, World Scientific, Singapore (1985).
- [16] *Generalized Coherent States and Their Applications*, by A. Perelomov, Springer-Verlag, New York (1986).
- [17] R. P. Feynman, Phys. Rev. **84**, 108 (1951).
- [18] P.B. Wiegmann, Phys. Rev. Lett. **60**, 821 (1988).
- [19] E. Witten, Nucl. Phys. **B223**, 422 (1983).
- [20] E. Brezin, S. Hikami, and J. Zinn-Justin, Nucl. Phys. **B165**, 528 (1980).
- [21] H. Levine, S.B. Libby and A.M.M. Pruisken, Nucl. Phys. **B240**, 30 (1984)
- [22] J. Brad Marston, private communication.
- [23] T. Dombre and G. Kotliar, preprint.
- [24] I. Affleck, T. Kennedy, E.H. Lieb, and H. Tasaki, Phys. Rev. Lett. **59**, 799 (1987); D.Arovas, A. Auerbach and F.D.M. Haldane, Phys. Rev. Lett. **60**, 531 (1988).
- [25] H. Bethe, Z. Phys. **71**, 205 (1931).

- [26] N. Read, unpublished
- [27] I. Affleck and F.D.M. Haldane, Phys. Rev **B36**, 5291 (1987)
- [28] I. Affleck, private communication
- [29] T. Ziman and H.J. Schulz, Phys. Rev. Lett. **59**, 140 (1987).
- [30] A.J. MacFarlane, Physics Letters **82B**, 239 (1979).
- [31] See *e.g. Solitons and Instantons*, by R. Rajaraman, North-Holland, Amsterdam (1982).

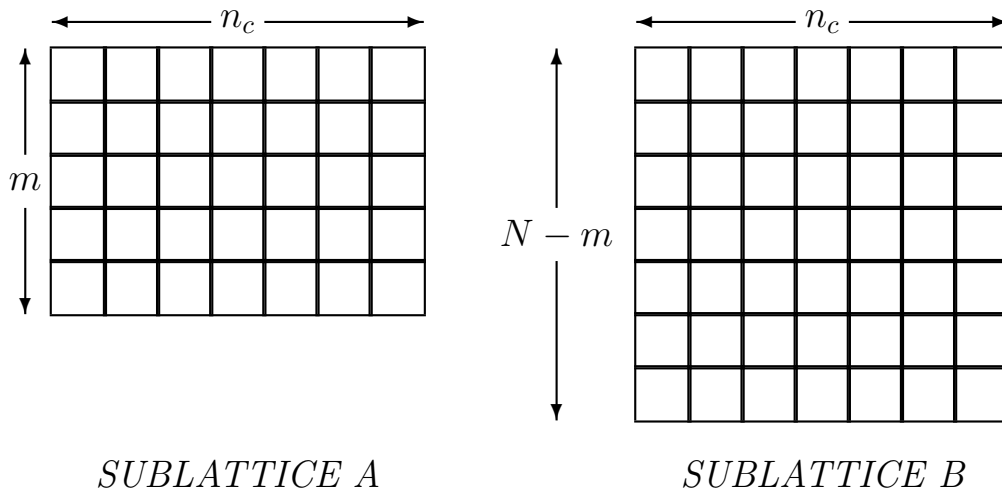


Figure 1. Young tableau of the $SU(N)$ representations by which the states on sites belonging to sublattice A and B transform.

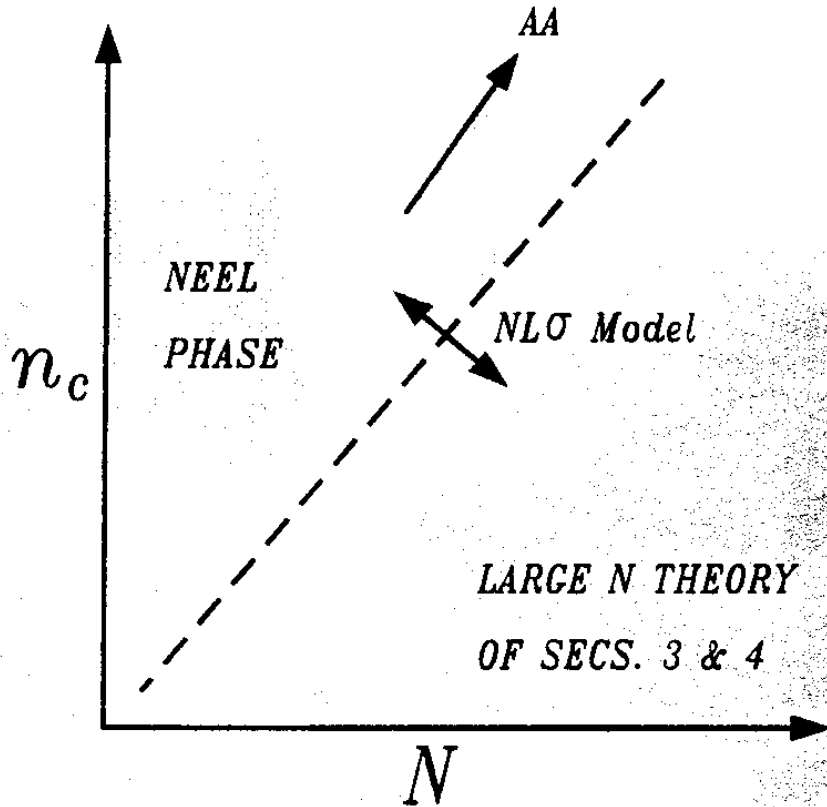


Figure 2. A constant m cross section of the phase diagram of the square lattice $SU(N)$ antiferromagnet. The dashed line represents a second order transition from the Neel phase to a spin-disordered state which is described by a (2+1) dimensional non-linear sigma ($NL\sigma$) model. The position of this line is insensitive to the value of m . The arrow labelled AA represents the region in which Auerbach and Arovas [6] analyzed the *bosonic* representation of the $SU(N)$ generators for the case $m = 1$.

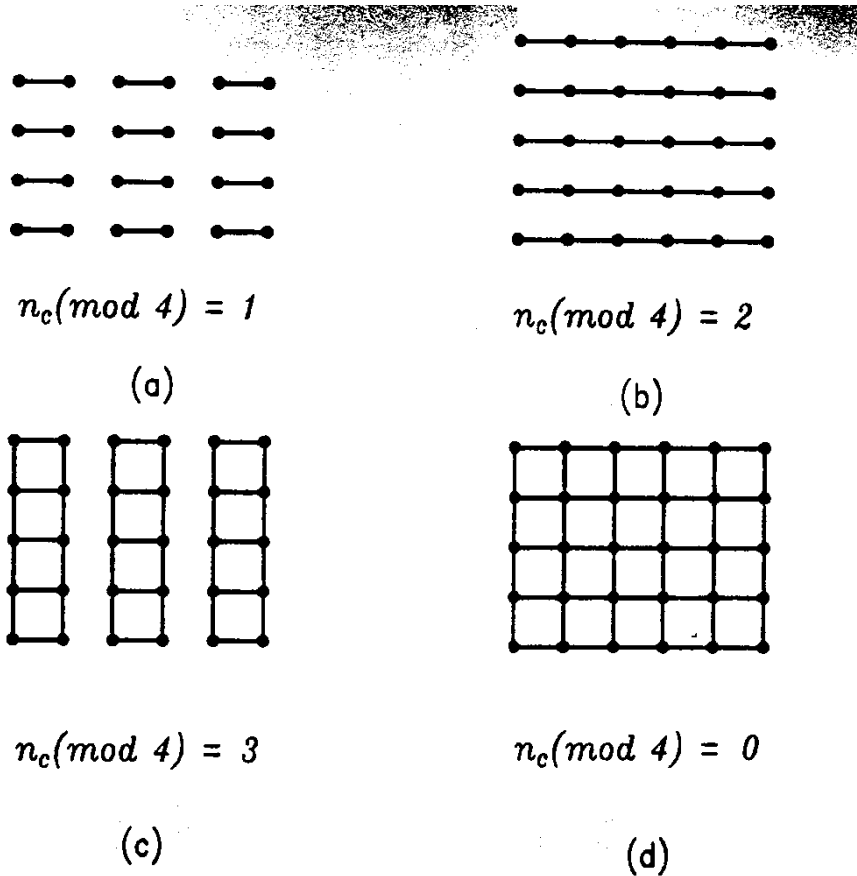


Figure 3. Metastable states of the Hamiltonian (1.1) for filling factor $m = N/2$ as a function of $n_c \pmod{4}$. The states chosen have the *minimum* possible degeneracy for their n_c value. Each line represents m singlet bonds between $SU(N)$ fermions on neighboring sites. There are n_c such bonds emerging from each site (Only the last $n_c \pmod{4}$ bonds are shown; the remaining form copies of the translationally invariant $n_c \pmod{4} = 0$ state).

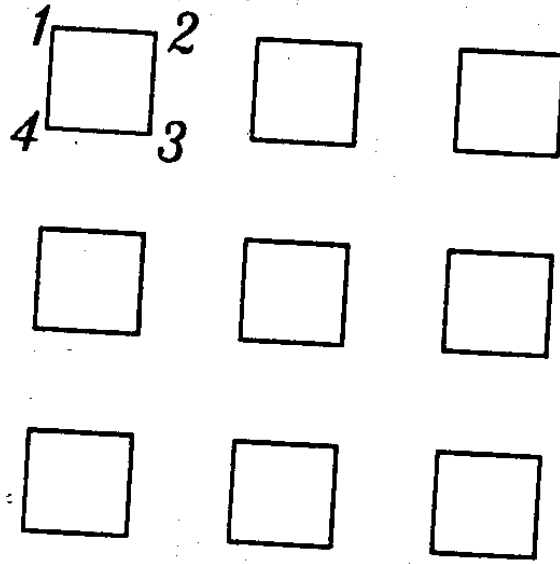


Figure 4. An example of the ‘plaquette’ states which is degenerate with the ‘bond’ states in the $N \rightarrow \infty$ limit.

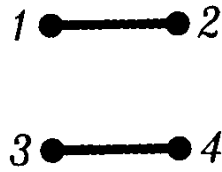


Figure 5. Bond configuration which leads to an off diagonal coupling between $\chi_a^a(13)$ and $\chi_a^a(24)$.

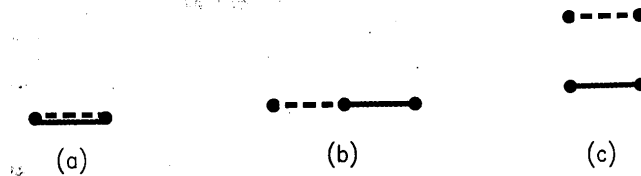


Figure 6. Local bond configurations which lead to off-diagonal couplings in the $\chi_b^a(ij)$ field. We represent bonds of color a by the thick line, and bonds of color b by the dashed line.

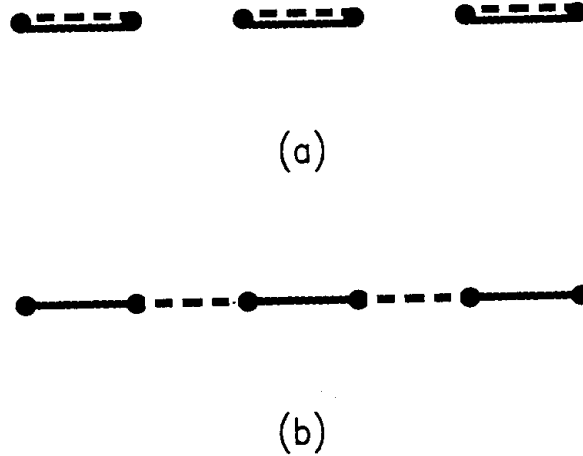


Figure 7. The two lowest configurations of bonds of colors a and b for a one-dimensional chain: (a) the ‘overlapping’ state and (b) the ‘alternating’ state (also the ground state)

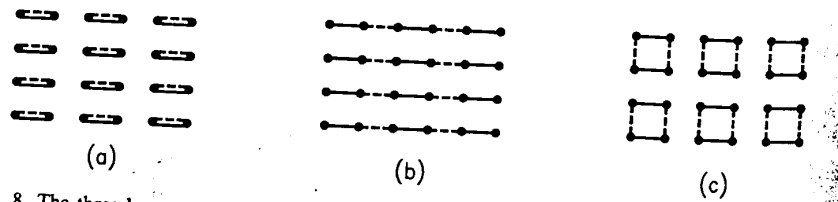
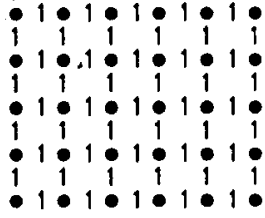


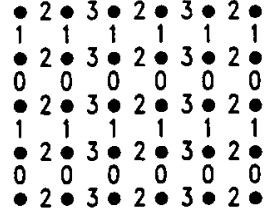
fig. 8. The three lowest configurations of bonds for $n_c = 2$ and $m = N/2$.

Figure 8. The three lowest configurations of bonds for $n_c = 2$ and $m = N/2$. The thick and dashed lines represent the two colors. Note that in all three states, the two colors are arranged in separate column states. The states are referred to as (a) the overlapping state, (b) the line state and (c) the square state.



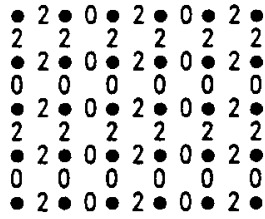
$$n_c = 4$$

(a)



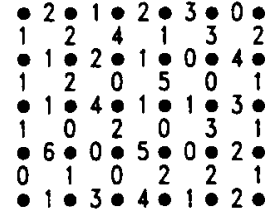
$$n_c = 6$$

(b)



$$n_c = 4$$

(c)



$$n_c = 7$$

(d)

Figure 9. Candidate ground states in the $N \rightarrow \infty$ limit for the case $m = 1$ for a variety of n_c values. The numbers on the links specify the number of bonds between the two sites. Note that the sum of the numbers on the four links ending at any site is always equal to n_c .

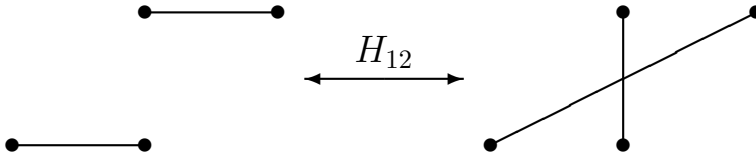


Figure 10. Fluctuations caused by the action of H_{12} upon a candidate ground state for $n_c = 1$. This fluctuation changes the energy at order $1/N^2$.

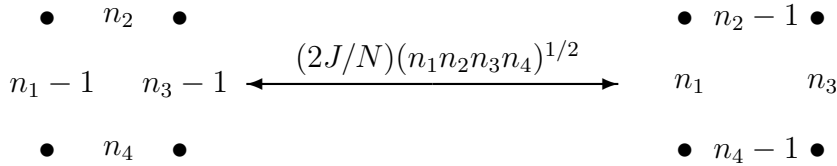


Figure 11. The off-diagonal term in H_{eff} which changes the local n_ℓ values on the links around a plaquette.

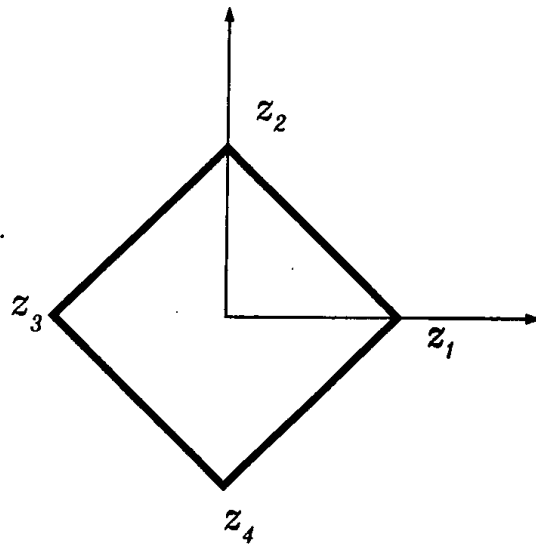


Figure 12. Four points surrounding the center of the skyrmion-number changing tunneling event which occurs at the origin. The light lines represent the x and y co-ordinate axis.